Migraine Complicated by Brachial Plexopathy as Displayed by MRI and MRA: Aberrant Subclavian Artery and Cervical Ribs

Ernestina H. Saxton, MD, PhD, Theodore Q. Miller, MD, and James D. Collins, MD
Los Angeles, CA

This article describes migraine without aura since childhood in a patient with bilateral cervical ribs. In addition to usual migraine triggers, symptoms were triggered by neck extension and by arm abduction and external rotation; paresthesias and pain preceded migraine triggered by arm and neck movement. Suspected thoracic outlet syndrome was confirmed by high-resolution bilateral magnetic resonance imaging (MRI) and magnetic resonance angiography (MRA) of the brachial plexus. An unsuspected aberrant right subclavian artery was compressed within the scalene triangle. The aberrant subclavian artery splayed apart the recurrent laryngeal and vagus nerves, displaced the esophagus anteriorly, and effaced the right stellate ganglia and the C8-T1 nerve roots. Scarring and fibrosis of the left scalene triangle resulted in acute angulation of the neurovascular bundle and diminished blood flow in the subclavian artery and vein. A branch of the left sympathetic ganglia was displaced as it joined the C8-T1 nerve roots. Left scalenectomy and rib resection confirmed the MRI and MRA findings; the scalene triangle contents were decompressed, and migraine symptoms subsequently resolved. (*J Natl Med Assoc.* 1999;91:333-341.)

Key words: ◆ aberrant subclavian artery ◆ brachial plexus ◆ migraine ◆ MRA ◆ MRI ◆ nerve imaging ◆ thoracic outlet syndrome

Migraine is a primary headache condition associated with blood flow changes in intracranial and extracerebral blood vessels. A typical attack of migraine without aura as defined by the International Headache Society consists of unilateral moderate to severe throbbing headache pain, with associated photophobia, phonophobia, nausea, and vomiting lasting from 4 to 72 hours.[1] Neck pain or stiffness often accompanies migraine even in mild attacks.[2-5] Patients report that neck pain as well as certain positions of the neck can trigger a migraine attack. Headache is reported to be one of the common complaints of thoracic outlet syndrome and may be a presenting symptom in some patients.[6]

Thoracic outlet syndrome is a disorder of the cervicothoracic spine caused by compression of the nerves and blood vessels supplying the upper limb.[7-12] Thoracic outlet disorders may involve dysfunction at the cervicothoracic level of the vertebral column, the first rib, the clavicle, the vascular supply, or adjacent soft tissues.[12] Symptoms often consist of upper extremity pain associat-

From the Departments of Neurology and Radiological Sciences, UCLA School of Medicine, Los Angeles, CA. Presented at the Annual Convention and Scientific Assembly of the National Medical Association, August 2-7, 1997, Honolulu, HI, and the Annual Meeting of the Federation of American Societies for Experimental Biology, April 22, 1998, San Francisco, CA. Requests for reprints should be addressed to Dr James D. Collins, Dept of Radiological Sciences, UCLA Medical Ctr, Ctr for the Health Sciences, Box 951721, Los Angeles, CA 90095-1721.

ed with numbness and tingling, radiating into the hands. Autonomic symptoms such as temperature and color changes may occur. Clinical diagnosis of thoracic outlet syndrome depends on general examination that may include such provocative tests as Adson's and hyperabduction maneuvers. Diagnostic noninvasive laboratory studies are indirect and involve conventional radiography and computerized tomography (CT). Computerized tomography may incorporate special software programs to display vascular anatomy. However, these CT vascular displays do not adequately demonstrate soft tissues. In addition, CT of the thorax is routinely performed with patient's arms overhead. In this position, the clavicle and the subclavius muscle compress the subclavian vein on the first rib (costoclavicular compression). Intrathoracic, intra-abdominal, and intracranial pressure increase under these conditions. When contrast is injected, collateral blood flow is develops at the site of venous compression. This should be considered in the interpretation of the results.

In patients with thoracic outlet syndrome, magnetic resonance imaging (MRI) typically is performed on the cervical spine to exclude cord lesions and radiculopathy. Multiplanar MRI and MRA display soft-tissue fascial planes. Bilateral brachial plexus MRI and vascular three-dimensional (3D) reconstruction imaging demonstrate the relationship of nerves and blood vessels to their surrounding landmark anatomy and delineate the sites of compromise without the need for contrast agent.[9,10,12]

In the past two years, more than 50 patients referred to our outpatient neurology clinic for evaluation of intractable migraine were found to have thoracic outlet complaints. In addition to headache symptoms, these patients reported paresthesias, temperature and color changes (especially in the hands), and pain in the neck, shoulder, and upper extremity. Clinical examination with arm abduction and external rotation resulted in loss of radial and brachial pulse with patients noting paresthesias, burning, arm pain or heaviness, and temperature changes. These maneuvers also triggered patients' typical migraine or headache symptoms.

The patient described in this article was one of the first cases evaluated by the authors. Her thoracic outlet syndrome symptoms and typical migraine attacks were triggered by driving, neck extension, and abduction and external rotation of the upper extremities.[13,14] This article demonstrates the sites of brachial plexus compression in a migraine patient with aberrant right subclavian artery, cervical ribs, and scarring and fibrosis of the left scalene triangle. Plain chest radiograph, selected sequential MRI, and 2D time-of-flight (TOF) MRA are displayed. Images that represent the landmark anatomy were selected; entire sequences for each plane could not be included in this article. The images selected were chosen because they complement each other as a group. Individual images were cross-referenced to the other sequences.

MATERIALS AND METHODS

Magnetic Resonance Imaging

Plain chest radiographs (PA and lateral) are obtained and reviewed prior to the bilateral brachial plexus MRI. The chest radiograph is obtained to detect osseous abnormalities and to eliminate the possibility of unsuspected metallic objects. Respiratory gating is applied throughout the procedure to minimize motion artifact and maximize the contrast of the soft-tissue signal intensities. The patient is positioned supine in the body coil with his or her arms down to the side.

A body coil is used because it offers optimal full field of view for bilateral imaging of the brachial plexus and provides uniform signal-to-noise ratio across the imaging field necessary for 3D reconstruction. Surface coils are limited to depth and field of view and are not adequate for bilateral imaging of the brachial plexus. A water bag (500 mL normal saline) is placed on the right and the left sides of the neck above the shoulder girdle to increase signal-to-noise ratio for higher resolution imaging. A full field of view (40-48 cm) of the neck and the thorax is used to image both supraclavicular fossae. A minimum of four imaging sequences is obtained: contiguous (4-5 mm) coronal, transverse (axial), transverse oblique, and sagittal T1-weighted images. If there is clinical evidence of scarring, tumor, or lymphatic obstruction, T2-weighted images or FSE (fast spin echo) pulse sequences are obtained.

The coronal sequence is imaged first. The brachial plexus envelops the artery, forming a neurovascular bundle. The nerves are best imaged when the cursors are aligned to the arterial blood supply. Because the margins of the axillary artery vary in each patient, the cursors must be adjusted individually for each bilateral MRI brachial plexus examination. The cursors are positioned from the skin surface of the posterior chest wall to the skin surface of the anterior chest wall for symmetry and 3D reconstruction as well as for detecting abnormalities that may mimic brachial plexopathies. The superior landmark is set at the base of the skull, and the inferior landmark is set at the level of the kidneys. The image that best demonstrates the arterial blood flow to the upper extremities is selected as the baseline image for the remaining sequences.

The transverse sequence is set from the baseline

coronal image at the superior aspect of the third cervical vertebral body to the carina. The lateral margins of the shoulder girdle are imaged to insure bilateral, simultaneous display of the brachial plexus.

The transverse oblique sequence is set by aligning the cursors to the arterial blood supply of each upper extremity using the baseline coronal sequence. The cursors are centered to the plane of the axillary artery, 2 cm below the inferior cord of the brachial plexus to the superior margin of the coracoid process. This sequence is necessary to detect signal intensity, architecture, and effacement of the long axis of the nerves, arteries, and veins.

The sagittal sequence is obtained by aligning the cursors laterally to the coracoid process and medially to include the insertion of the anterior scalene muscle on the first rib and the middle third of the first thoracic vertebral body. The sagittal plane is necessary to detect effacement of the neurovascular bundle by the coracoid process, pectoralis minor muscle, clavicle and subclavius muscle, axillary masses, and abnormalities of the scalene triangle.

Coronal abduction and external rotation sequence displays the posteroinferior rotation of the clavicles and subclavius muscles on the landmark anatomy of the neck and shoulder girdle. After completion of the 2D TOF MRA sequence, the patient is removed from the gantry, and without changing body position, the patient's arms are abducted and extended behind the head. The patient is then returned to the gantry. This sequence is imaged from the posterior level of the first thoracic nerve roots to the anterior margin of the manubrium sterni and first ribs to display the rotation of the clavicles in relationship to anatomic landmarks. The sagittal abduction-external rotation sequence is imaged from the lateral margin of the left coracoid process to the lateral margin of the right coracoid process. The images are then cross-referenced to the above imaging sequences. The clavicles and subclavius muscles rotate posterior inferiorly (18°-53°) and compress the neurovascular bundles against the first ribs. The coronal and sagittal abduction-external rotation sequences capture images that demonstrate changes in the relationship of the neurovascular bundles to the position of the clavicles.

When an image sequence is completed, it is transferred to another screen at an independent workstation for review and 3D-reformat display. The software for this 3D reconstruction is already in a 1.5-Tesla GE Signa MRI unit (GE Medical Systems, Milwaukee, WI). The images are stored on CT and MRI (GE9800) format and on optical disks for 3D-color reconstruction on the ISG workstation (ISG Technologies Inc, Mississauga, Ontario, Canada). The entire study is monitored by the radiologist and requires 90 minutes. Selected Kodak color and black-and-white laser prints and transparencies are obtained for lectures and poster presentations, and annotated images are preserved on VHS and archived digital optical disks.

Equipment

Magnetic resonance images are obtained on the 1.5-Tesla GE Signa MR scanner. The 3D-reformatted images are videotaped on a separate work console at the monitoring station, and computerized color is applied to the images using an ISG console. A 512×256-matrix format is used. The saline water bags are those supplied for intravenous use.

CASE REPORT

A 36-year-old, right-handed woman presented for evaluation of worsening migraine headache. She reported a history of headaches since childhood characteristic of migraine without aura. After menarche, her migraines became more frequent and severe, with the most severe episodes occurring on the left side. No association with the menstrual cycle occurred until she started oral contraceptive medication at age 18 years. The migraine attacks became more severe at the time of menses and were incapacitating during pregnancy. The headaches became less frequent and more manageable after a total abdominal hysterectomy and bilateral salpingo-oopherectomy at age 22.

The patient reported that during the previous three years, since began training as a physical therapist, the migraines had increased in frequency and severity, and were associated with neck pain and tightness. The migraines were triggered more easily by alcohol, aromatic scents such as perfumes and cologne, sunlight and heat, and lunchmeat. The frequent headaches were preceded by "pins and needles" and a tingling sensation in both hands, mainly in the ring and little fingers, as well as aching in the forearms. These arm symptoms were brought on by activities such as prolonged sitting or extending the neck when having her hair washed at the hairdresser. Symptoms were the most severe after arm abduction and external rotation, and the worst headaches were left-sided, occurring 5-20 minutes after precipitation of arm symptoms by these maneuvers. The severe attacks also were associated with debilitating nausea, vomiting, and photophobia.

Both of the patient's parents had a history of migraines. A physical examination revealed positive hyperextension and Adson's tests that were greater on the

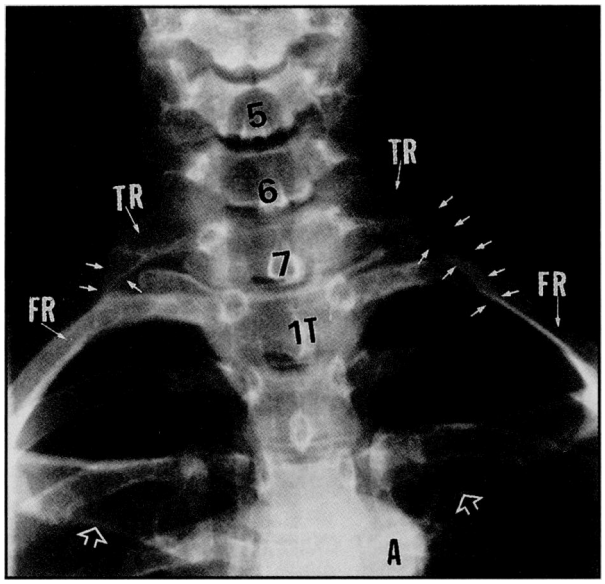

Figure 1.
Coned down PA chest radiograph demonstrates bilateral cervical ribs. The small right cervical rib originates from the transverse process of C7 and overlies the posterior first rib. The larger left cervical rib crosses the high transverse process of the first thoracic vertebra, posterior first rib, and plura. The right shoulder girdle is low. (5=fifth cervical vertebra; 6=sixth cervical vertebra; 7=seventh cervical vertebra; 1T=first thoracic vertebra; arrows=right cervical rib [3 arrows] and left cervical rib [8 arrows]; open arrows=clavicles; A=aorta; TR=transverse process of C7.)

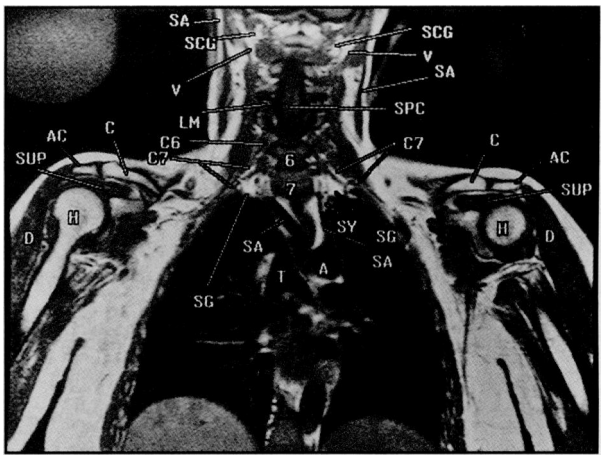

Figure 2.
Coronal sequences demonstrating the aberrant subclavian artery originating from the left descending aorta and ascending posterior to the esophagus and trachea and effacing the right stellate ganglia. The right and left common carotid arteries originate from the aorta. (A=aorta; AC=acromion; C=clavicle; C6-C7=nerve root; D=deltoid; H=humerus; SA=subclavian artery; SCG=superior cervical ganglion; SG=stellate ganglion; SPC=spinal cord; SUP=supraspinatus muscle; SY=sympathetic nerve; T=trachea; V=vagus nerve; 6=sixth cervical vertebra; 7=seventh cervical vertebra; LM=lateral mass [pillar] of vertebral body.)

left than on the right side. These maneuvers produced obliteration of the radial pulse on the left and diminution on the right, with sensory complaints in the hands and pain in the arms. Several minutes after these procedures, the patient reported headache and nausea. A neurologic examination revealed mild weakness of finger abduction (digiti minimi), finger extension, and elbow extension in both extremities, but greater on the left. Decreased vibration sense was found on the left compared to the right, with deep tendon reflexes more forthcoming on the left than on the right. Chest radiographs demonstrated bilateral cervical ribs, with the left being larger than the right (Figure 1).

Bilateral MRI and MRA of the brachial plexus were requested to demonstrate the site of brachial plexus compromise. The large left cervical rib crossed the higher transverse process of the first thoracic vertebral body. An aberrant right subclavian artery was discovered on the coronal MRI sequence (Figure 2). The artery originated from the left descending aorta and ascended obliquely posterior to the esophagus and trachea, anterior to the first thoracic and seventh cervical vertebral bodies over the posterior apex of the pleura. The artery effaced the stellate ganglia over the posterior aspect of the pleura and was compressed in the scalene triangle by the large right anterior scalene muscle. The right C7 cervical nerve root was displaced anteriorly by the cervical rib. The left subclavian artery entered the scalene triangle over the low first rib. The large left middle scalene muscle displaced the C5, C6, and C7 cervical nerve roots anteriorly as they coursed over the cervical rib into the supraclavicular fossa. These nerve roots were straightened and their signal intensity diminished.

Transverse sequence confirmed the aberrant right subclavian artery originating from the aortic arch. The artery narrowed within the scalene triangle as it arched acutely over the first rib. There was acute angulation and compression of the left neurovascular bundle posterior to the anterior scalene muscle. The left C8-T1 nerve roots were crimped by the dilated subclavian artery. The left transverse oblique sequence confirmed the acute

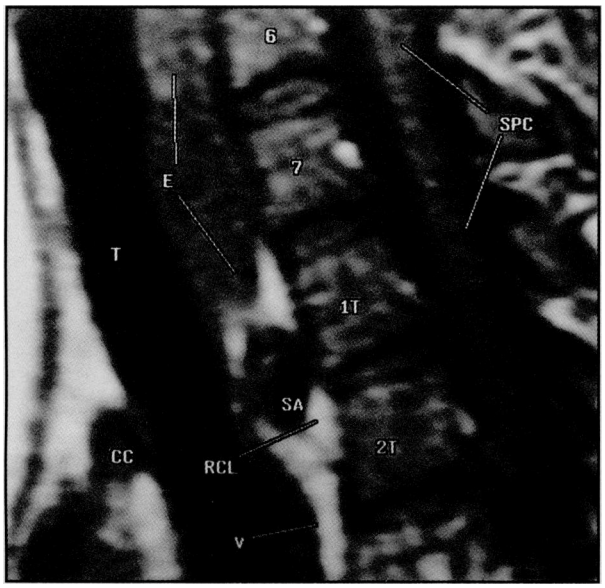

Figure 3.
Sequential right sagittal image demonstrating ascent of the aberrant subclavian artery as it courses posterior to the esophagus and trachea, passing the first and second thoracic vertebral bodies. The artery is in the retroesophageal space, impinging the vagus nerve. (6=sixth cervical vertebra; 7=seventh cervical vertebra; 1T=first thoracic vertebra; 2T=second thoracic vertebra; CC=common carotid artery; E=esophagus; T=trachea; SA=subclavian artery; SPC=spinal cord; RCL=recurrent laryngeal nerve; and V=vagus nerve.)

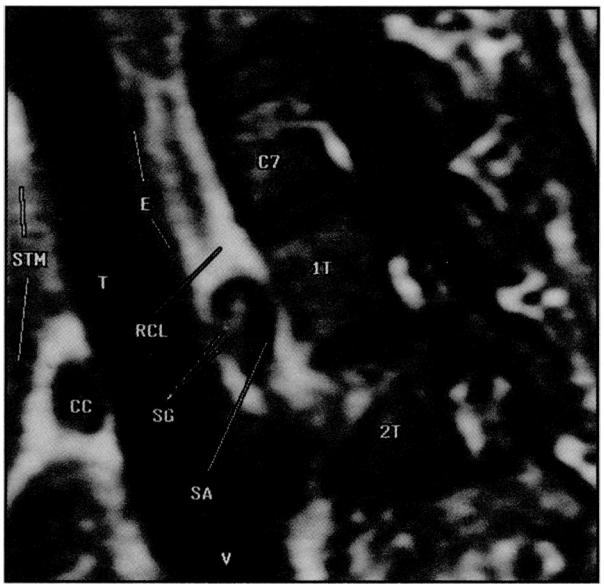

Figure 4.
Sequential right sagittal image demonstrating continued ascent of the aberrant subclavian artery splaying the vagus and recurrent laryngeal nerves anterior to the first and second thoracic vertebral bodies. (C7=seventh cervical vertebra; 1T=first thoracic vertebra; 2T=second thoracic vertebra; CC=common carotid artery; E=esophagus; T=trachea; SA=subclavian artery; RCL=recurrent laryngeal nerve; V=vagus nerve; SG=stellate ganglion; and STM=sternocleidomastoid muscle.)

angulation of the left neurovascular bundle. The left cervical rib was identified anterior and lateral to the transverse process of C7 as it coursed anteriorly over the intercostal nerve of the first thoracic vertebral body. A branch of the sympathetic ganglia was displaced by the lung anterior-medially as it joined the C8-T1 nerve roots. The right transverse oblique sequence confirmed the dilatation of the aberrant subclavian artery and the effacement of the T1 nerve root as it coursed anteriorly. The C8-T1 nerve roots crossed the pleura binding to the dilated subclavian artery. The artery was compressed as it passed between the anterior and middle scalene muscles and narrowed lateral to the anterior scalene.

The right sagittal sequence demonstrated the retroesophageal position of the narrowed aberrant subclavian artery (Figures 3 and 4). The artery bisected the vagus and right recurrent laryngeal nerves (Figure 4), descended into the scalene triangle, and effaced the stellate ganglia (Figures 5 and 6). The artery invaginated the lung and displaced the C8-T1 nerve roots superiorly.

Coronal bilateral abduction and external rotation of the upper extremities confirmed the origin of the aberrant subclavian artery from the descending left aorta (Figure 7). The artery was dilated proximal to the scalene triangle and was compressed within the triangle. The low right clavicle and the subclavius muscle compressed the neurovascular bundle against the hemithorax. On the left, intermediate gray signal intensities (fibrosis and scarring) marginated the neurovascular bundle. Two-dimensional TOF-reconstructed MRA images displayed the origin of the aberrant subclavian artery from the descending aorta (Figure 8). The images demonstrated proximal dilatation of the left axillosubclavian vein, partial compression of the right axillosubclavian vein, and compression of the aberrant subclavian artery within the scalene triangle. An amorphous high-signal intensity was displayed over the region of the left scalene triangle consistent with collateral circulation.

With MRI anatomic correlation, the patient underwent left surgical decompression. This consisted of transaxillary first dorsal rib resection and resection of the

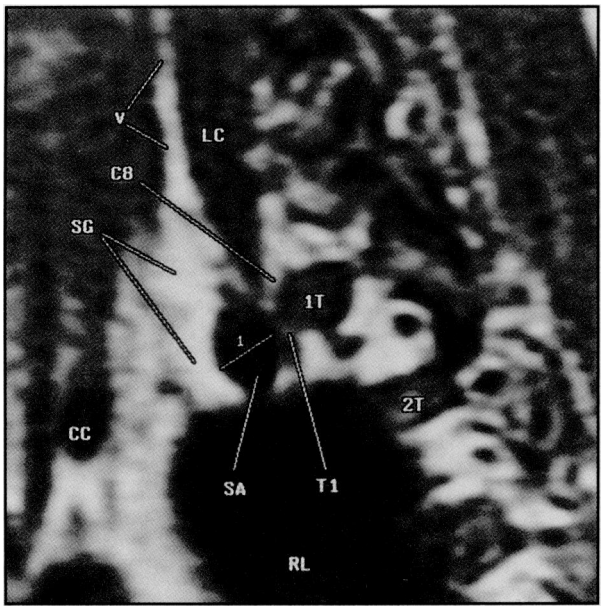

Figure 5.
Sequential right sagittal image demonstrating the aberrant subclavian artery beginning its course over the pleural of the right lung. The stellate ganglion is effaced and displaced superolaterally. (1T=first thoracic vertebra; 2T=second thoracic vertebra; C8=C8 cervical nerve root; CC=common carotid artery; LC=longus colli muscle; RL=right lung; SA=subclavian artery; SG=stellate ganglion; and V=vagus.; T1=first thoracic nerve root; 1=measurement of diameter of subclavian artery [8 mm].)

Figure 6.
Sequential right sagittal image demonstrating the aberrant artery compressed anterior to the first thoracic vertebra body, coursing over and invaginating the pleura on the right and displacing the stellate ganglion superior laterally. (C8=C8 cervical nerve root; R1=first rib; T1=T1 nerve root; IP=invaginated pleura; LC=longus colli muscle; RL=right lung; SA=subclavian artery; SG=stellate ganglion; SY=sympathetic nerve and trunk; and V=vagus nerve; 1=measurement of diameter of subclavian artery [7 mm].)

left cervical rib, subtotal anterior and middle scalenectomy, lysis of the left axillosubclavian artery and vein, and neurolysis of the inferior trunk and T1 nerve root of the brachial plexus. At surgery, extensive abnormalities of the left thoracic outlet were observed. There was complete intercostalization of the scalene muscles with a large muscle mass filling the concavity of the first rib superiorly. The cervical rib arose from the C7 transverse process and ended at the junction of the T1 nerve root and inferior trunk of the brachial plexus, deviating the brachial plexus anteriorly and causing a groove in the nerve components in that region. The cervical rib was enveloped in the intercostal muscle with a large attachment to the middle scalene muscle. A fibrocartilaginous band was observed above the cervical rib that appeared to arise from the transverse process of the C6 body on the left. This band was attached to the first rib at the termination of the cervical rib and further deviated the brachial plexus. Crossing fibers constricted the axillosubclavian vessels that arose from the intercostalized scalene muscle (Figure 7). The cervical rib indented the inferior trunk of the brachial plexus and had to be elevated from the trunk prior to resection.

The intercostalized scalene muscle also contributed constricting bands across the axillosubclavian vessels, the inferior trunk, and the T1 nerve root, all of which were lysed after sectioning of the muscle. Surgical decompression resulted in resolution of the intractable migraines.

DISCUSSION

The patient described here had a history of headache since childhood, which fulfilled the International Headache Society criteria for migraine without aura.[1] Of significance was the fact that in addition to usual triggers, the patient's migraine symptoms were triggered by positions of the neck and arms that caused thoracic outlet neurovascular compression. The migraine was preceded by paresthesias in the hands and pain in the arms that were greater on the left than the right. On

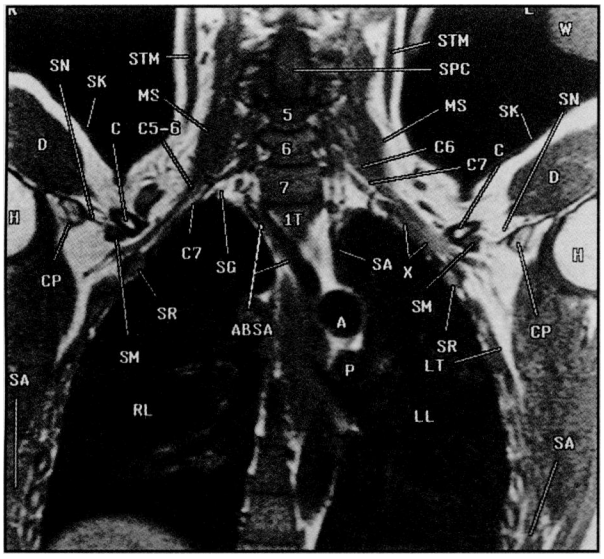

Figure 7.
Coronal abduction and external rotation of the upper extremities demonstrate the aberrant subclavian artery and the left clavicle and subclavius muscle compressing the neurovascular bundle on the left. (A=aorta; ABSA=aberrant subclavian artery; C=clavicle; CP=coracoid process; D=deltoid muscle; H=humerus; LL=left lung; LT=long thoracic nerve; MS=middle scalene muscle; RL=right lung; SG=stellate ganglion; SK=skin; SM=subclavius muscle; SPC=spinal cord; STM=sternocleidomastoid muscle; 5=fifth cervical vertebra; 6=sixth cervical vertebra; 7=seventh cervical vertebra; 1T=first thoracic vertebra; C5-C6=junction of fifth and sixth cervical nerve roots; C6=sixth cervical nerve root; C7=seventh cervical nerve root; P=pulmonary artery; SA=subclavian artery; SN=suprascapular nerve; SR=second rib; W=saline water bag; X=site of fibrosis and scarring of the neurovascular bundle with intermediate gray signal intensities.)

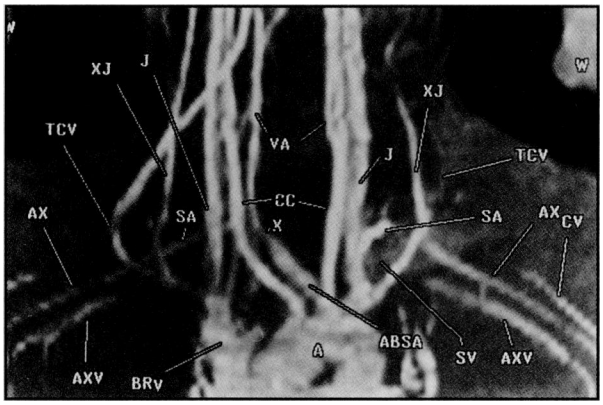

Figure 8.
Coronal reconstruction 2D TOF MRA demonstrates proximal dilatation of the left axillosubclavian vein, partial compression of the right axillosubclavian vein, collateral flow on the left side, and the aberrant subclavian artery as it narrows within the right scalene triangle. (A=aorta; ABSA=aberrant subclavian artery; AX=axillosubclavian artery; AXV=axillosubclavian vein; BRV=brachiocephalic vein; CC=common carotid artery; J=internal jugular vein; SA=subclavian artery; SV=subclavian vein; TCV=transverse cervical vein; VA=vertebral artery; XJ=external jugular vein; X=site of compression of aberrant subclavian artery; CV=cephalic vein; W=saline water bag.)

physical examination, provocative maneuvers including abduction and external rotation of the upper extremities triggered a migraine attack.

The chest radiograph demonstrated bilateral cervical ribs (Figure 1). The MRI and MRA studies demonstrated abnormalities of the thoracic outlet. These included bilateral cervical ribs and compression of the neurovascular structures, especially on the left, by the large cervical and first ribs as well as the middle scalene muscle. The MRI and MRA studies also displayed the presence and course of an aberrant right subclavian artery. The aberrant subclavian artery effaced the esophagus and splayed apart the recurrent laryngeal and vagus nerves in the retroesophageal space. It effaced the stellate ganglia and was compressed within the scalene triangle (Figures 3-6). The pressure on the recurrent laryngeal nerve and esophagus with the impingement in the retroesophageal space most likely accounted for the patient's reports of episodes of hoarseness and dysphagia.

The coronal abduction-external rotation sequence triggered upper bilateral extremity pain and paresthesias that were greater on the left than the right. A migraine followed the upper extremity symptoms while the patient was still in the gantry and worsened after she exited the imaging unit. Abduction-external rotation MRI demonstrated compression of the neurovascular bundle bilaterally at the time of the triggered symptoms (Figure 7). The captured images provided the clinician with a record of the anatomic dysfunction that correlated with the patient's presenting symptoms.

Surgical decompression confirmed the neurovascular anomalies displayed on the MRI and MRA. Prior to surgery, the patient underwent scalene block, which was positive and consistent with thoracic outlet syndrome. However, in subsequent patients to be reported, MRI and MRA of the brachial plexus were used as the sole anatomic correlation to determine surgical decompression, in the absence of electrophysiologic studies such as evoked potentials, electromyography, nerve conduction,

or other invasive studies such as scalene block.

The relationship of migraine to neurovascular compression associated with structural abnormalities of the thoracic outlet was documented by MRI techniques. This was achieved by the radiologist monitoring the entire bilateral MRI and MRA of the brachial plexus. Functional anatomic imaging also was possible by abduction and external rotation of the upper extremities in the MRI gantry, which duplicated the same symptoms that occurred in the physician's office. Abduction-external rotation of the upper extremities caused the clavicles and subclavius muscles to rotate posteroinferiorly and compress the subclavian vein and the soft tissues anterior to the scalene triangles (Figure 7). This pressure was transmitted to the scalene triangle, triggering the patient's symptoms (costoclavicular compression).[12] Abduction-external rotation of the upper extremities increases intrathoracic pressure, causes venous obstruction, and increases interscalene triangle compression, which trigger paresthesias, pain, and migraine.[12,13]

Intracranial and extracerebral blood flow changes are postulated to contribute to migraine pain.[15,16] Compression of the blood vessels in the thoracic outlet not only produces local blood flow changes,[17,18] but also may contribute to impairment of cerebral vascular reactivity and blood flow, with resultant migraine pain and symptoms. Additionally, autonomic changes also may contribute to the vascular changes that accompany migraine. Thoracic outlet patients often present clinically with autonomic changes, especially changes in sympathetic tone, in the extremities, and MRI demonstrates compression of the brachial plexus.[18] In the patient described here, in addition to neurovascular compression, the stellate ganglia were compromised and the sympathetic nerves displaced. Stellate ganglion blockade has been postulated to be associated with blood flow changes and precipitating migraine pain and symptoms in certain patients.[19,20]

Thus, abnormalities in sympathetic tone may have contributed to changes in blood vessel reactivity and to blood flow changes that induced migraine pain. Surgical first rib resection and scalenectomy to decompress the neurovascular structures resolved the autonomic symptoms and brachial plexus complaints. In this patient, the surgical procedure also resolved the intractable migraine symptoms and resulted in less frequent attacks and better response to migraine medications.

Definitive conclusions about the pathogenesis of migraine cannot be made from this clinical and MRI study. It is likely that both vascular and neurogenic mechanisms are involved in the complex disorder that is migraine. Since the first presentation of this study in 1997, we have evaluated more than 50 patients with intractable headache; patients' symptoms were directly related to neurovascular and autonomic abnormalities of the thoracic outlet. In these patients, who were subjects of a subsequent study, maneuvers that produce neurovascular compromise triggered their migraine complaints.[21] In these patients, bilateral abduction external rotation MRI sequence demonstrated changes consistent with increased intraabdominal and intracerebral pressures as well as increased intrathoracic pressure. Impaired venous flow was demonstrated as increased signal intensities within the internal jugular, subclavian, brachiocephalic, and innominate veins, at the same time that the patients complained of triggered migraine symptoms while in the MRI gantrly.[21,22] Venous obstruction and impaired venous drainage of the head and neck contributed to migraine symptoms in these patients.

Knowledge of anatomy is important in understanding and interpreting MRI and MRA studies in patients.[23] An important anatomic finding in this patient was the course of the aberrant right subclavian artery from its origin from the descending aorta to its retroesophageal position, with splaying apart of the vagus and recurrent laryngeal nerves and effacement of the stellate ganglia not previously reported.

CONCLUSION

Neurovascular compression in a migraine patient with thoracic outlet abnormalities triggered migraine attacks. Surgical decompression resulted in resolution of the intractable migraine. High-resolution multiplanar bilateral MRI and MRA of the brachial plexus provided definitive diagnostic anatomic modalities in surgical management of a TOS patient with migraine.[21] The usefulness of bilateral MRI and MRA in delineating compression abnormalities of the brachial plexus and in surgical management of this patient was evident (even in the absence of conventional electrophysiologic studies and invasive studies such as scalene block). Magnetic resonance imaging displayed the anatomic finding not previously reported of an aberrant right subclavian artery splaying apart the vagus and recurrent laryngeal nerves in the retroesophageal space and effacement of the stellate ganglia.

Literature Cited

1. Headache Classification Committee of the International Headache Society. Classification and diagnostic criteria for headache disorders, cranial neuralgias and facial pain. *Cephalalgia.* 1988;8(suppl 7):10-73.

2. Edmeads J. The cervical spine and headache. *Neurology.* 1988;38:1874-1878.

3. Vernon H, Steiman I, Hagino C. Cervicogenic dysfunction in muscle contraction headache and migraine: a descriptive study. *J Manipulative Physiol Ther.* 1992;15:418-429.

4. Kidd RF, Nelson R. Musculoskeletal dysfunction of the neck in migraine and tension headache. *Headache.* 1993;33:566-569.

5. Blau N, MacGregor MB. Migraine and the neck. *Headache.* 1994;34:88-90.

6. Raskin NH, Howard MW, Ehrenfeld WK. Headache as the leading symptom of thoracic outlet syndrome. *Headache.* 1985;25:208-210.

7. Sunderland S. Blood supply of the nerves to the upper limb in man. *Arch Neurol Psych.* 1945;53:91-115.

8. Lord JW, Rosati LM. Thoracic outlet syndromes. *Clin Symp.* 1971;23:1-32.

9. Collins JD, Shaver M, Disher AC, Miller TQ. Compromising abnormalities of the brachial plexus as displayed by magnetic resonance imaging. *Clin Anat.* 1995;8:1-16.

10. Collins JD, Disher AC, Miller TQ. The anatomy of the brachial plexus as displayed by magnetic resonance imaging: technique and applications. *J Natl Med Assoc.* 1995;87:489-498.

11. Thompson JF, Jannsen F. Thoracic outlet syndromes. *Br J Surg.* 1996;83:435-436.

12. Collins JD, Shaver M, Disher A, Miller TQ. The costoclavicular syndrome as displayed by MRI and MRA: reformat and 3D graphic display. *Clin Anat.* 1997;10:131.

13. Saxton EH, Collins JD, Miller TQ. Migraine complicated by brachial plexopathy: Aberrant subclavian artery and cervical ribs. Presented at: Annual Convention and Scientific Assembly of the National Medical Association; August 2-7, 1997; Honolulu, HI.

14. Saxton E, Collins JD, Disher A, Miller TQ. Migraine complicated by brachial plexopathy as displayed by MRI and MRA. *FASEB J.* 1998;12:A1110.

15. Harer C, vonKummer R. Cerebrovascular CO2 reactivity in migraine: assessment by transcranial Doppler ultrasound. *J Neurol.* 1991;238:23-26.

16. Thomsen LL, Iversen HK, Olesen J. Cerebral blood flow velocities are reduced during attacks of unilateral migraine without aura. *Cephalalgia.* 1997;15:109-116.

17. Collins JD, Shaver ML, Disher A, Miller TQ. The vascular supply of the brachial plexus as displayed by magnetic resonance imaging: magnetic resonance angiography (MRA). Presented at: 11th Annual Scientific Program of the American Association of Clinical Anatomists; June 16, 1994; Galveston, TX.

18. Saxton EH, Collins JD, Disher A, Miller TQ. Migraine complicated by brachial plexopathy as displayed by magnetic resonance imaging (MRI) and magnetic resonance angiography (MRA). Presented at: Annual Convention and Scientific Assembly of the National Medical Association; August 1-6, 1998, New Orleans, LA.

19. Lehman LJ, Warfield CA, Bajwa ZH. Migraine headache following stellate ganglion blockade for reflex sympathetic dystrophy. *Headache.* 1995;36:335-337.

20. Uyemaya T, Kugimiya T, Ogawa T, Kandori Y, Ishizuka A, Hanaoka K. Changes in cerebral blood flow estimated after stellate ganglion block by single-photon emission computed tomography. *J Auton Nerv Syst.* 1995;50:339-346.

21. Saxton EH, Collins JD, Miller TQ. Migraine complicated by brachial plexopathy as displayed by MRI and MRA. Presented at: 15th Annual Scientific Program of the American Association of Clinical Anatomists; June 9-13, 1998; Lexington, KY.

22. Saxton EH, Collins JD, Ahn S, Miller TQ. Venous obstruction in brachial plexopathy as displayed by MRI, MRA, and 3D reconstruction in migraine patients with thoracic outlet syndrome. *FASEB J.* 1999;12:A676.

23. Collins JD, Shaver ML, Disher AC, Miller TQ. Bilateral magnetic resonance imaging of the brachial plexus and peripheral nerve imaging; technique and three-dimensional color. In: Omer GE, Spinner M, Van Beek AL. *Management of Peripheral Nerve Problems.* 2nd ed. Philadelphia, PA: WB Saunders Co; 1998:82-93.